

Choice of Thresholding Technique in Micro-CT Images of Trabecular Bone Does Not Influence the Prediction of Bone Volume Fraction and Apparent Modulus

Chi Hyun Kim^{1,2}, Byung Gwan Kim¹, X. Edward Guo³

¹Department of Biomedical Engineering, Yonsei University, Wonju, Kangwon Do, Korea

²Institute of Medical Engineering, Yonsei University, Wonju, Kangwon Do, Korea

³Department of Biomedical Engineering, Columbia University, New York, NY 10027, USA

(Received January 17, 2007. Accepted April 2, 2007)

Abstract

Trabecular bone can be accurately represented using image-based finite element modeling and analysis of these bone models is widely used to predict their mechanical properties. However, the choice of thresholding technique, a necessary step in converting grayscale images to finite element models which can thus significantly influence the structure of the resulting finite element model, is often overlooked. Therefore, we investigated the effects of thresholding techniques on micro-computed tomography (micro-CT) based finite element models of trabecular bone. Three types of thresholding techniques were applied to micro-CT images of trabecular bone which resulted in three unique finite element models for each specimen. Bone volume fractions and apparent moduli were predicted for each model and compared to experimental results. Our findings suggest that predictions of apparent properties agree well with experimental measurements regardless of the choice of thresholding technique in micro CT images of trabecular bone.

Key words : micro-computed tomography, finite element analysis, thresholding, bone volume fraction, apparent modulus

I. INTRODUCTION

Mechanical properties of trabecular bone depend on its microstructural parameters such as the bone volume fraction(BVF) and connectivity. Biomechanical characterization of trabecular bone, especially its structure-function relationship will contribute to the better understanding of the etiology of age-related fractures.

High resolution micro-computed tomography(micro-CT) and micro-magnetic resonance imaging(micro-MRI) are non-invasive imaging techniques to quantify the complex three-dimensional(3D) architecture of trabecular bone[1-5]. Micro finite element(FE) models based on these high resolution images have become a widely used tool for the study of trabecular bone mechanics and adaptation[6-19]. It has been shown in several studies that these micro FE models of trabecular bone can provide relatively accurate predictions in

elastic modulus and yield strength[6,7,9-12]. In most of these analyses, the original digital images of trabecular bone have to be thresholded to distinguish between bone and bone marrow voxels with only bone voxels converted into elements used in the finite element model. Choice of threshold value is critical as small variations in the threshold value can significantly influence the predicted bone volume fraction and mechanical properties[19]. The thresholding technique used in this procedure may also have significant impact on the accuracy of these micro FE models.

In this study, the effects of thresholding techniques on micro-CT image based finite element models were investigated. Using bovine trabecular bone specimens, the apparent elastic moduli were first determined by performing uniaxial compression tests. These trabecular bone specimens were then scanned using a micro-CT and converted into finite element models using three thresholding techniques : (1) adaptive thresholding, (2) global thresholding, and (3) BVF-matched global thresholding. Finite element analyses were performed to obtain predicted apparent moduli. The effects of various thresholding techniques on the BVF and predicted apparent modulus were examined and compared to experimental measurements.

This study is supported in part by grants from the Yonsei University Research Fund of 2005 and Whitaker Foundation.

Corresponding Author : Dr. Chi Hyun Kim
Department of Biomedical Engineering, Yonsei University
234 Maejiri, Wonju, Kangwon Do, Korea
Tel : +82-33-760-2785 / Fax : +82-33-760-2197
E-mail : chihyun@yonsei.ac.kr

II. MATERIALS AND METHODS

Ten freshly frozen bovine proximal tibiae were obtained from a local slaughter house and cut into 12 mm thick coronal sections using a band saw. Contact radiographs were taken from these sections and 12 mm x 40 mm rectangular regions of trabecular bone were identified such that the principal orientation of the trabeculae was aligned (qualitatively by inspection) with the longitudinal axis of the rectangle. The radiographs were placed on the corresponding tibiae sections and the identified trabecular regions (12 mm × 12 mm × 40 mm) were cut using a band saw. Under wet conditions, seventeen 8.6 mm diameter and 40 mm long cylinders were cored out from these trabecular bone blocks. The ends of the cylindrical bone specimens were cleaned of bone marrow using a water jet and embedded with adhesive in internally threaded brass end caps using a custom-made alignment jig [20]. The specimens were frozen in -80°C and while the specimens were still frozen the diameter of the mid-span of each specimen was reduced to 6 mm with a gage length of 10 mm using a lathe. The diameter of each specimen was measured using a digital caliper three times with its average reported. Uniaxial compression tests were performed using a servo-hydraulic material testing machine (MTS810, MTS, Minneapolis, MN) with an 8 mm gage length extensometer (632.26F-20, MTS, Minneapolis, MN) mounted on the gage region of the specimen. A 2500 N load transducer (661.18E-02, MTS, Minneapolis, MN) was used to record the load. Specimens were tested under strain control with a rate of 0.0005 s⁻¹ up to 0.8% strain with care taken such that the specimens were not compressed past the ultimate strength. The testing control and data acquisition were performed using the TestStar IIS software (MTS, Minneapolis, MN). The stress was determined by dividing the load by the cross-sectional area of the specimen. The apparent elastic modulus was obtained from the linear region of the stress-strain curve (0.0%-0.1% of strain). After mechanical testing, the central gage region (8 mm length) of each specimen was cut and the length measured using the digital caliper three times with its average reported. The bone marrow from the gage region was removed using water jet cleaning and ultrasonic bath. Both the wet weight and the submerged weight (measured while submerging specimens under water) of each sample were measured. The apparent density was calculated by dividing the wet weight by the specimen apparent volume while the bone tissue density was determined by Archimedes's principle. The BVF was calculated by dividing the apparent density by the bone tissue density.

The gage region of each specimen was scanned using a

micro-CT system (μ CT 20, Scanco Medical, Switzerland) at 34 μ m nominal resolution. Each 3D micro-CT image was segmented using a low-pass filter to remove noise. Binarized digital models were constructed using three types of thresholding techniques: adaptive, global, and BVF-matched global. In adaptive thresholding, throughout the 3D image, local (adaptive) thresholds were obtained in local volumes depending on the grayscale value of the surrounding voxels [3]. In global thresholding, a unique threshold value was selected based on the histogram distribution of the 256 gray values in the 3D image of each specimen. The minimum gray value between bone and background peaks in the histogram was used as the threshold value. Any voxel with a grayscale value above this threshold was considered as a bone voxel while any voxel with a grayscale value equal to or below the threshold was reset to a gray value of zero. A third set of thresholded images ("BVF-matched global") was also processed by adjusting the global threshold value, such that the BVF matched the BVF obtained through physical density measurements.

Thresholded 3D images were converted to 3D linearly elastic finite element models by mapping each bone voxel to an 8-node brick element. The models were solved using an element-by-element pre-conditioned conjugate gradient solver [21]. The isotropic bone tissue modulus was set as 18 GPa and Poisson's ratio as 0.3 [22]. The apparent modulus of the specimen were obtained from models constructed using each of the thresholding methods. The BVF and apparent modulus resulting from each thresholding technique were compared to the values obtained through experiment using a paired Student's t-test (Systat, SPSS Science, Chicago, IL).

III. RESULTS

Different thresholding techniques on micro-CT images of bovine trabecular bone specimens resulted in three different voxel-based 3D finite element models for each specimen. Visually, the resulted images from the global and adaptive thresholding were similar while the "matched global" produced different images, especially in areas of bone with dramatic variations in trabecular thickness (Fig. 1).

All three methods produced models with BVF that were not significantly different ($p > 0.05$) from BVF obtained through density measurements while the predicted values from all three models have good correlations with the experimentally measured values ($r^2 > 0.93$) (Fig. 2). BVF ranged between 8% and 35%.

The apparent elastic moduli of the specimens determined from the linear region of the stress-strain curve obtained from mechanical testing were in the range of 500 to 5000 MPa.

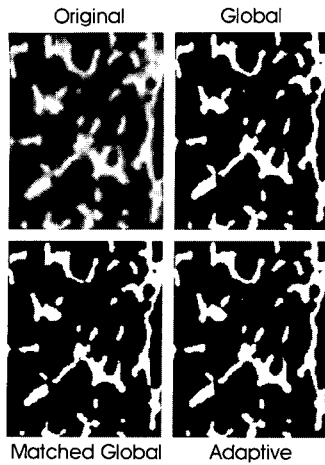


Fig. 1. Typical section of an 8-bit micro-CT image of bovine trabecular bone before and after three different types of thresholding.

Similar to the BVF, the apparent moduli calculated from the three methods were not significantly different ($p > 0.05$) from the apparent modulus obtained through mechanical testing with good correlations with the experimental measurements ($r^2 > 0.91$) (Fig. 3).

IV. DISCUSSION

In this study, three types of thresholding methods (*i.e.*, global, adaptive, and matched global) were applied to micro-CT images of bovine trabecular bone. BVF and apparent elastic moduli were calculated from image-based FE models and compared to those measured directly from physical density measurements and mechanical testing. Results from this study revealed that all three thresholding methods on

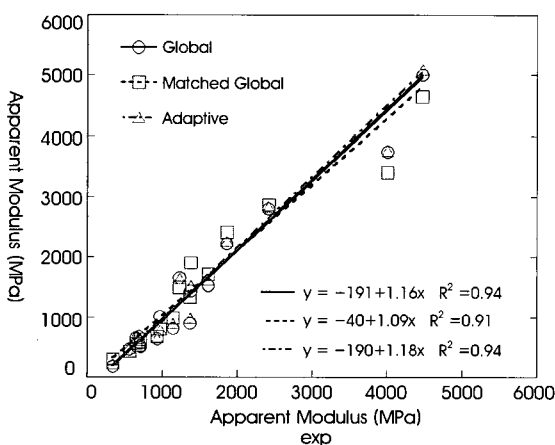


Fig. 3. Apparent modulus predicted by finite element models after different types of thresholding correlated to apparent modulus from mechanical testing.

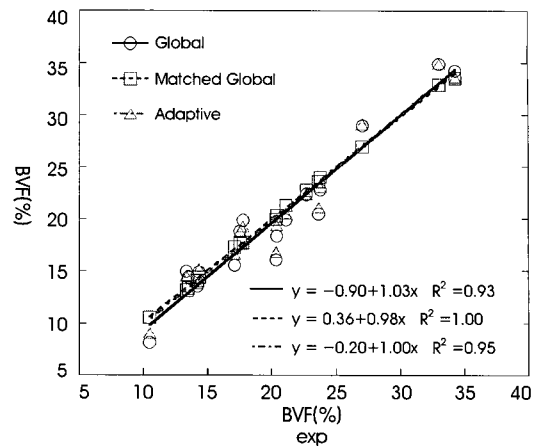


Fig. 2. BVF predicted by finite element models after different types of thresholding correlated to BVF from physical density measurements.

micro-CT images have no significant effect on BVF and apparent moduli. Upon qualitative inspection of the thresholded images along with the original micro-CT image, there were clear variations in local trabecular bone morphology depending on thresholding technique (Fig. 1). Thin trabeculae are more likely to have grayscale values that are closer to values of background compared to thicker trabeculae. As a result, these thin trabeculae are more sensitive to the threshold value and can be inadvertently converted to background that leads to a disruption in the connectivity of trabecular bone. This may lead to a modification in trabecular bone morphology where the difference can be detected only at the local tissue level. However, it appears that the different outcomes of trabecular morphology are minimal, at least at the apparent level, considering BVF and apparent moduli comparisons produced results not significantly different from experimental results. These results support previous studies that have used either one of the three thresholding methods compared in this study to determine the trabecular bone properties at the apparent level [3,9,11,13-15].

When extrapolating these results, one must keep in mind that this study was performed on bovine trabecular bone. It is possible that the results from this study may have to be validated when analyzing different animals, such as rat or mouse where their trabeculae are thinner compared to bovine trabecular bone used in this study. Also, thresholding of whole bone that includes both the trabecular and cortical bone may pose different problems. The choice of thresholding technique may be more crucial in these cases although further studies are needed.

Although the choice of thresholding technique did not affect the overall statistical outcome of this study, one must

take into account that there are individual images, especially those with lower bone density, that are more sensitive to the change in threshold value and technique. This implies that there may be individual oversights in image-based bone density measurements, especially in patients with lower bone density (and thus more likely to develop bone fractures) depending on the thresholding technique applied. In addition, image quality (e.g., signal-to-noise ratio or micro-CT resolution) which was not compared in this study may have an effect on the overall outcome. Therefore, the choice of thresholding technique should not be overlooked when examining individual grayscale images trabecular bone.

REFERENCES

- [1] S. Majumdar and H.K. Genant, "Assessment of trabecular structure using high resolution magnetic resonance imaging," *Stud. Health Technol. Inform.*, vol. 40, pp. 81-96, 1997.
- [2] S. Majumdar, H.K. Genant, S. Grampp, D.C. Newitt, V.H. Truong, J.C. Lin, and A. Mathur, "Correlation of trabecular bone structure with age, bone mineral density, and osteoporotic status: in vivo studies in the distal radius using high resolution magnetic resonance imaging," *J. Bone Miner. Res.*, vol. 12, pp. 111-118, 1997.
- [3] J.L. Kuhn, S.A. Goldstein, L.A. Feldkamp, R.W. Goulet, and G. Jesion, "Evaluation of a microcomputed tomography system to study trabecular bone structure," *J. Orthop. Res.*, vol. 8, pp. 833-842, 1990.
- [4] P. Ruegsegger, B. Koller, and R. Muller, "A microtomographic system for the nondestructive evaluation of bone architecture," *Calcif. Tissue Int.*, vol. 58, pp. 24-29, 1996.
- [5] J.A. Hipp, A. Jansujwicz, C.A. Simmons, and B.D. Snyder, "Trabecular bone morphology from micro-magnetic resonance imaging," *J. Bone Miner. Res.*, vol. 11, pp. 286-297, 1996.
- [6] B. van Rietbergen, S. Majumdar, W. Pistoia, D.C. Newitt, M. Kothari, A. Laib, and P. Ruegsegger, "Assessment of cancellous bone mechanical properties from micro-FE models based on micro-CT, pQCT and MR images," *Technol. Health Care*, vol. 6, pp. 413-420, 1998.
- [7] B. Van Rietbergen, R. Muller, D. Ulrich, P. Ruegsegger, and R. Huiskes, "Tissue stresses and strain in trabeculae of a canine proximal femur can be quantified from computer reconstructions," *J. Biomech.*, vol. 32, pp. 165-173, 1999.
- [8] J.P. van den Bergh, G.H. van Lenthe, A.R. Hermus, F.H. Corstens, A.G. Smals, and R. Huiskes, "Speed of sound reflects Young's modulus as assessed by microstructural finite element analysis," *Bone*, vol. 26, pp. 519-524, 2000.
- [9] G.L. Niebur, M.J. Feldstein, J.C. Yuen, T.J. Chen, and T.M. Keaveny, "High-resolution finite element models with tissue strength asymmetry accurately predict failure of trabecular bone," *J. Biomech.*, vol. 33, pp. 1575-1583, 2000.
- [10] G.L. Niebur, J.C. Yuen, A.J. Burghardt, and T.M. Keaveny, "Sensitivity of damage predictions to tissue level yield properties and apparent loading conditions," *J. Biomech.*, vol. 34, pp. 699-706, 2001.
- [11] G.L. Niebur, J.C. Yuen, A.C. Hsia, and T.M. Keaveny, "Convergence behavior of high-resolution finite element models of trabecular bone," *J. Biomech. Eng.*, vol. 121, pp. 629-635, 1999.
- [12] B. Borah, G.J. Gross, T.E. Dufresne, T.S. Smith, M.D. Cockmar, P.A. Chmielewski, M.W. Lundy, J.R. Hartke, and E.W. Sođ, "Three-dimensional microimaging (MRmicroI and microCT), finite element modeling, and rapid prototyping provide unique insights into bone architecture in osteoporosis," *Anat. Rec.*, vol. 265, pp. 101-110, 2001.
- [13] G.T. Charras and R.E. Guldberg, "Improving the local solution accuracy of large-scale digital image-based finite element analyses," *J. Biomech.*, vol. 33, pp. 255-259, 2000.
- [14] D. Ulrich, T. Hildebrand, B. Van Rietbergen, R. Muller, and P. Ruegsegger, "The quality of trabecular bone evaluated with micro-computed tomography, FEA and mechanical testing," *Stud. Health Technol. Inform.*, vol. 40, pp. 97-112, 1997.
- [15] D. Ulrich, B. van Rietbergen, H. Weinans, and P. Ruegsegger, "Finite element analysis of trabecular bone structure: a comparison of image-based meshing techniques," *J. Biomech.*, vol. 31, pp. 1187-1192, 1998.
- [16] R.E. Guldberg, S.J. Hollister, and G.T. Charras, "The accuracy of digital image-based finite element models," *J. Biomech. Eng.*, vol. 120, pp. 289-295, 1998.
- [17] A.J. Ladd, J.H. Kinney, D.L. Haupt, and S.A. Goldstein, "Finite-element modeling of trabecular bone: comparison with mechanical testing and determination of tissue modulus," *J. Orthop. Res.*, vol. 16, pp. 622-628, 1998.
- [18] J. Homminga, R. Huiskes, B. Van Rietbergen, P. Ruegsegger, and H. Weinans, "Introduction and evaluation of a gray-value voxel conversion technique," *J. Biomech.*, vol. 34, pp. 513-517, 2001.
- [19] T. Hara, E. Tanck, J. Homminga, and R. Huiskes, "The influence of microcomputed tomography threshold variations on the assessment of structural and mechanical trabecular bone properties," *Bone*, vol. 31, pp. 107-109, 2002.
- [20] T.M. Keaveny, X.E. Guo, E.F. Wachtel, T.A. McMahon, and W.C. Hayes, "Trabecular bone exhibits fully linear elastic behavior and yields at low strains," *J. Biomech.*, vol. 27, pp. 1127-1136, 1994.
- [21] S.J. Hollister, J.M. Brennan, and N. Kikuchi, "A homogenization sampling procedure for calculating trabecular bone effective stiffness and tissue level stress," *J. Biomech.*, vol. 27, pp. 433-444, 1994.
- [22] X.E. Guo and S.A. Goldstein, "Is trabecular bone tissue different from cortical bone tissue?" *Forma*, vol. 12, pp. 185-196, 1997.